

Control of laser-beam spatial distribution for correcting the shape and refraction of eye cornea

O.I. Baum, A.I. Omelchenko, E.M. Kasianenko, R.V. Skidanov, N.L. Kazanskiy, E.N. Sobol', A.V. Bolshunov, S.E. Avetisov, V.Ya. Panchenko

Abstract. The results of calculation and development of a device aimed at forming a laser beam with an annular intensity distribution and spatial mode homogenisation, as well as approbation of this device for biological phantoms and eyes in *ex vivo* experiments with laser non-ablative correction of the cornea profile, are presented. The radiation intensities and thermal field distributions on the surfaces of a phantom and isolated rabbit's eye are investigated. The absence of significant heating in the central region of eye is confirmed. It is shown that this device can be used for laser impact in order to change symmetrically eye's refraction.

Keywords: laser, refraction, annular intensity distribution, eye cornea, correction.

1. Introduction

Eye diseases are known to lead often to visual impairments [1]. These impairments are caused by the changes occurring in the elements of the optomechanical system of human eye, such as cornea, crystalline lens, etc. In some cases, these changes are corrected using additional optical elements (glasses, contact lenses, etc.) [2] or performing surgical interference to correct the refraction of individual elements [3] and recover or replace these elements; an example is the replacement of crystalline lens with intraocular lenses (IOLs) [4].

Recently, certain progress has been made in refraction medicine due to the application of ortokeratology [5]. However, overnight wear of contact lenses, which is used in keratology, recovers the normal eye refraction for only a short time. The local thermomechanical effect of laser radiation on a cornea beyond its optical region leads to a more lasting change in refraction [6–8]. Note also that some new diagnostic methods based on optical coherence tomography have been developed for the last few years. These methods make it possible to

investigate the fine features of thermomechanical change in the eye cornea shape [9, 10] and slow deformations occurring after the laser impact [11]. Successive irradiation of a series of points on the surface of cornea (symmetric relative to its paracentral area) [12] may lead to asymmetry of cornea tension in the optical zone and thus cause side effects (astigmatism, keratoconus, etc.) when treating diseases by ablation methods [3]. This problem can be solved using one-shot irradiation by a beam with a symmetric intensity profile.

The lasers used in ophthalmologic operations (erbium-doped solid-state or diode-pumped fibre lasers) are characterised by insufficiently stable spatial intensity distribution [13, 14], which is due (as preliminary studies showed) to the nonuniform intensity distribution in different spatial modes and instability of laser beam transmission system. This is a hindrance for clinical tests and further practical application of the new method for eye refraction correction in ophthalmology.

Different optical elements and schemes have been used to form a laser beam with annular intensity distribution: reflecting cylindrical mirrors, lens optics, free-form surfaces, axicons, and diffractive optical elements (DOEs) synthesised based on computer calculations [15]. The devices based on the so-called focusers [15–17] turned out to be the most efficient ones (from the point of view of laser energy conversion and quality of annular energy distribution). The elements of such kind are being improved [18, 19]. In particular, implementation of specified illuminance on a curvilinear surface using a free-form refracting element was considered in [19]. However, all aforementioned approaches have drawbacks. It is generally assumed that a plane wave, or a Gaussian beam, or a beam of a more complex shape (but with a known intensity distribution) [19] is incident on the optical element forming a specified intensity distribution. The initial beam is transformed in a special way (generally with a large loss of power) in optical experiments. If the beam shape is far from ideal or even unknown, the distribution formed by it may differ significantly from the calculated one.

In this paper, we present a modification of the calculation method based on the Gerchberg–Saxton (GS) algorithm, which makes it possible to form a light ring with a highly uniform intensity distribution due to the partition of the DOE region into segments and individual calculation of the element phase function for each segment. The results of the development of a device for forming a laser beam with an annular intensity distribution and homogenised spatial modes are presented. The final purpose of this study is to implement a laser impact, to investigate the intensities of radiation and thermal fields on the eye surface in *ex vivo* experiments using modes of non-ablative laser correction of cornea profile implemented in the developed device, and to estimate the

O.I. Baum, A.I. Omelchenko, E.M. Kasianenko, V.Ya. Panchenko
Institute of Photon Technologies, Federal Scientific Research Centre 'Crystallography and Photonics', Russian Academy of Sciences, ul. Pionerskaya 2, 142190 Troitsk, Moscow, Russia;
e-mail: baumolga@gmail.com;

R.V. Skidanov, N.L. Kazanskiy Institute of Image Processing Systems, Federal Scientific Research Centre 'Crystallography and Photonics', Russian Academy of Sciences, ul. Molodogvardeiskaya 151, Samara, 443001 Russia;

E.N. Sobol' Arcuo Medical, Inc., Los Altos, 94022 California, USA;
A.V. Bolshunov, S.E. Avetisov Research Institute of Ocular Diseases, ul. Rossolimo 11A, Moscow, 119021 Russia

Received 4 December 2019

Kvantovaya Elektronika 50 (1) 87–93 (2020)

Translated by Yu.P. Sin'kov

potential of this method in laser operations aimed at changing the cornea refraction.

2. Experimental

The instruments used in the experiments were as follows: a solid-state diode-pumped laser LAKhTA-MILON (St. Petersburg, Russia) with a wavelength $\lambda = 1.56 \mu\text{m}$; fluorescent IR detectors FID-AS-22 (OJSC Polironik, Moscow, Russia) for converting the energy of IR radiation into visible light (i.e., visualising IR radiation); a laser beam power distribution profile meter based on a CCD camera with a VGA resolution of 640×480 , connected to a computer with image processing software; an optical fibre $600 \mu\text{m}$ in diameter (Avantes, USA); refractive converters of the laser beam intensity distribution (VOLO, St. Petersburg, Russia); and similar diffractive converters (Institute of Image Processing Systems, Russian Academy of Sciences, Samara, Russia).

To reduce the influence of light scattering in fluorescent converters when measuring the radiation intensity distribution in transmitted light, thin fluorescent films were fabricated. A laser beam was directed to a film and then (after passing through a green filter GF-1) to a CCD camera. The laser power was measured by a power meter (Field-master Coherent, Inc., USA).

The photothermal effect of laser radiation on eye cornea models (gel spheres) was estimated using an infrared imager Testo 875-1 (TESTOSE & CO, KGA, Lenzkirch, Germany). Laser radiation with a special form of intensity distribution after an annular converter was directed onto the surface of a sphere 10 mm in diameter. The thermal radiation from the heated spherical surface was focused using an IR objective onto the sensitive surface of a detecting infrared imager.

3. Formation of a laser beam with an annular intensity distribution

The transformation of a laser beam with a rectangular intensity distribution and nonuniform filling of modes into a beam with an annular intensity distribution is based on the synthe-

sis of a DOE that transforms inhomogeneous radiation at the laser output into homogeneous one. Figure 1 shows the initial intensity distribution for a laser beam consisting of six transverse modes, measured at a distance of 100 mm from the laser output connector.

A calculation of a DOE forming a specified annular distribution at a specified distance from the DOE plane is reduced to the search for the phase transmission function of the element that would form a specified annular intensity distribution in the lens focal plane disregarding the phase distribution obtained in the output plane. This problem can be solved using various iterative methods [20–24], e.g., the Gerchberg–Saxton method. The main advantage of iterative algorithms is that they are more exact as compared with other algorithms for DOE phase calculation. At the same time, one must take into account that the elements obtained by these methods have an irregular microrelief in most cases, which imposes stricter requirements on their fabrication technology [20, 21].

3.1. Gerchberg–Saxton algorithm

The GS algorithm is aimed at solving the nonlinear integral Fresnel equation, which is used to calculate the optical elements forming an arbitrary specified intensity distribution of coherent monochromatic light in some plane oriented perpendicular to the optical axis [18]. A new estimate of the desired function in each iteration is chosen not only in correspondence with the desired intensity function but also in dependence of the previous estimate. The algorithm convergence rate depends on the choice of specific values of some weighting or regularisation parameters. Furthermore, we will consider the conventional GS algorithm without introducing any weighting parameters.

Within the scalar theory of diffraction, the complex amplitude of wave in the (u, v) plane of the optical element,

$$W(u, v) = A(u, v)\exp[i\phi(u, v)] \quad (1)$$

is related to the wave complex amplitude in the (ξ, η) image plane,

$$F(\xi, \eta) = B(\xi, \eta)\exp[i\psi(\xi, \eta)]. \quad (2)$$

In the formation plane of the desired intensity distribution we have

$$F(\xi, \eta) = \frac{ik}{2\pi z} e^{ikz} \times \int_{-\infty}^{\infty} \int_{-\infty}^{\infty} W(u, v) H(u - \xi, v - \eta, z) du dv, \quad (3)$$

where

$$H(u - \xi, v - \eta, z) = \exp\left\{\frac{ik}{2z}[(u - \xi)^2 + (v - \eta)^2]\right\} \quad (4)$$

is the impulse response function of free space in the Fresnel approximation, z is the distance between the DOE and observation plane, and k is the wave number. Within the Fraunhofer approximation the impulse response function of free space takes the form

$$H(u - \xi, v - \eta, z) = \exp[ik(u\xi + v\eta)]. \quad (5)$$

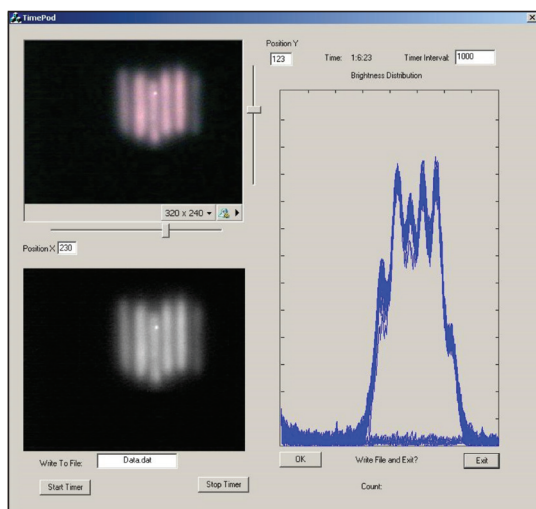


Figure 1. Intensity distribution in a laser beam at the output of a diode-pumped solid-state laser: (left) mode spatial distribution and (right) intensity distribution profile.

Within the approximation of thin optical element (transparency approximation), which disregards the ray refraction, the complex amplitude W in Eqn (3) is the product of complex amplitude $W_0(u, v)$ by the transmission eigenfunction $T(u, v)$ of the DOE:

$$W(u, v) = W_0(u, v)T(u, v). \quad (6)$$

Since the approximation in use considers only phase optical elements, the DOE transmission function was chosen in the form

$$T(u, v) = \exp[i g(u, v)], \quad (7)$$

where $g(u, v)$ is the specified DOE phase.

The calculation of the phase function $g(u, v)$ can be reduced to solution of the nonlinear integral equation

$$\begin{aligned} I_0(\xi, \eta) &= |F(\xi, \eta)|^2 \\ &= \left| \frac{k}{2\pi z} \int_{-\infty}^{\infty} \int_{-\infty}^{\infty} A_0(u, v) e^{i\phi(u, v)} H(u - \xi, v - \eta, z) du dv \right|^2, \end{aligned} \quad (8)$$

where $I_0(\xi, \eta)$ is the specified intensity in the image region. The image formation scheme using a DOE is shown in Fig. 2.

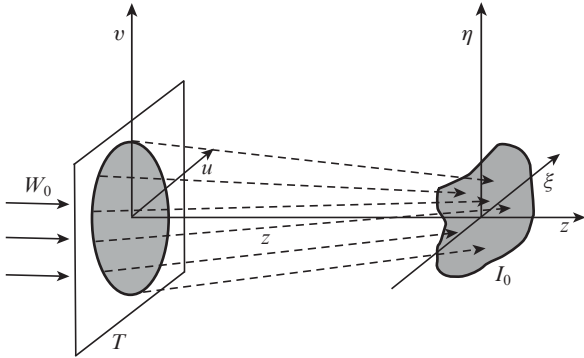


Figure 2. Schematic of image formation using a DOE.

The iterative method for calculating the phase $\phi(u, v)$ and, correspondingly, the phase $g(u, v)$, implies solution of Eqn (8) by the method of successive approximations. The GS (or error reduction) algorithm includes the following steps:

(1) an initial estimate is chosen arbitrarily for the phase $\phi_0(u, v)$;

(2) integral transformation of the function $W_0 = A_0(u, v) \times \exp[i\phi_0(u, v)]$ is performed according to formula (3);

(3) the thus obtained complex amplitude $F(\xi, \eta)$ in the image formation plane is replaced with the complex amplitude $\bar{F}(\xi, \eta)$ according to the rule

$$\bar{F}(\xi, \eta) = B_0(\xi, \eta) F(\xi, \eta) |F(\xi, \eta)|^{-1}, \quad (9)$$

where $B_0(\xi, \eta) = \sqrt{I_0(\xi, \eta)}$;

(4) the transform inverse to (3) relative to the function $\bar{F}(\xi, \eta)$ is calculated:

$$\begin{aligned} W(u, v) &= \frac{ik}{2\pi z} e^{-ikz} \\ &\times \int_{-\infty}^{\infty} \int_{-\infty}^{\infty} \bar{F}(\xi, \eta) H^*(\xi - u, \eta - v, z) d\xi d\eta; \end{aligned} \quad (10)$$

(5) the found complex amplitude $W(u, v)$ in the DOE plane is replaced with $\bar{W}(u, v)$ according to the rule

$$\bar{W}(u, v) = \begin{cases} A_0(u, v) W(u, v) |W(u, v)|^{-1}, & (u, v) \in Q, \\ 0, & (u, v) \notin Q, \end{cases} \quad (11)$$

where Q is the form of the DOE aperture;

(6) transition to step 2.

This procedure is carried out until errors δ_F and δ_W , which are defined as

$$\delta_F^2 = \frac{\int_{-\infty}^{\infty} \int_{-\infty}^{\infty} [|F(\xi, \eta)| - B_0(\xi, \eta)]^2 d\xi d\eta}{\int_{-\infty}^{\infty} \int_{-\infty}^{\infty} B_0^2(\xi, \eta) d\xi d\eta}, \quad (12)$$

$$\delta_W^2 = \frac{\int_{-\infty}^{\infty} \int_{-\infty}^{\infty} [|W(u, v)| - A_0(u, v)]^2 du dv}{\int_{-\infty}^{\infty} \int_{-\infty}^{\infty} A_0^2(u, v) du dv}, \quad (13)$$

become slightly varying values. The GS algorithm convergence is characterised by the stagnation effect: the error δ_F (or δ_W) rapidly decreases during several initial iterations, and all subsequent iterations do not lead to any significant decrease in it.

The modification of the GS algorithm performed in this study concerns the calculation domain of the element phase function. The above-described algorithm was successively applied to six segments (Fig. 3).

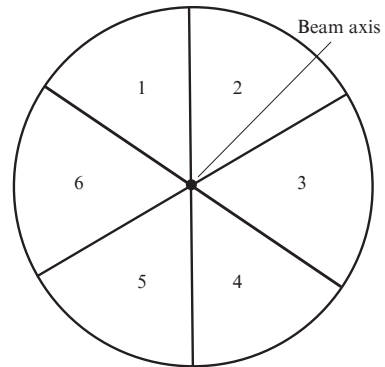


Figure 3. DOE segmentation aimed at forming an annular distribution.

Each segment in Fig. 3 was calculated as a completely independent element, focusing beam into a ring. The calculation was performed on the assumption that the initial beam had a Gaussian intensity distribution. The joint application of six individual focusing elements (even at a significantly asymmetric shape of the initial beam and error in centring the element in the output plane, one can obtain highly uniform illuminance in the light ring.

3.2. Calculation of DOE output parameters

The DOE model is a pattern of relief, which is deposited on glass (or some other similar material). Generally, images of phase transmission functions are calculated in the form of black and white images with 255 shades of gray. The white and black colours correspond to the areas with the largest and zero phase relief heights, respectively. When going from white to black colour, the relief is decreased by a value of $\lambda/(n-1)$, where λ is the laser wavelength, and n is the refractive index of the DOE material. Therefore, the phase of the radiation transmitted through DOE changes by 2π from white to black segments. Figure 4 shows (a) the DOE phase calculated according to the GS algorithm when the intensity distribution is formed as a light ring in the Fraunhofer approximation and (b) the intensity distribution itself.

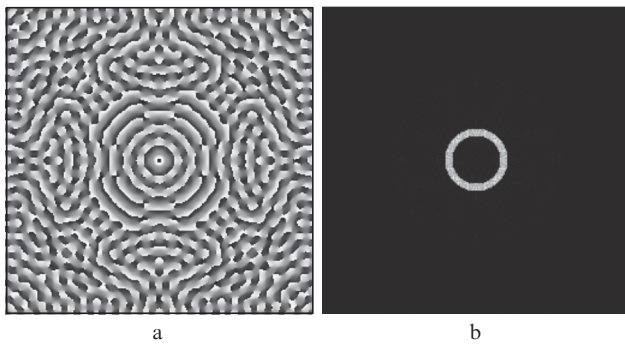


Figure 4. DOE calculation based on the GS algorithm: (a) DOE phase and (b) ring image.

Figure 5 presents a converter of the radiation intensity distribution, which uses the optical element calculated according to above-described algorithm. The converter changes the laser beam intensity distribution shown in Fig. 1 into an annular distribution (Fig. 6). Note that the laser radiation (inhomogeneous in space) had a rectangular intensity distribution for each of the six spatial modes, was unstable in time, and depended on the emitted power.

The ring converter (see Fig. 5) is mounted on a fibre connected to a LAKhTA-MILON laser. The radiation at the converter output had an annular distribution. Two distributions of laser beam intensity, shown in Figs 6a and 6b, respectively, were obtained using a fluorescent converter FID-AS-22

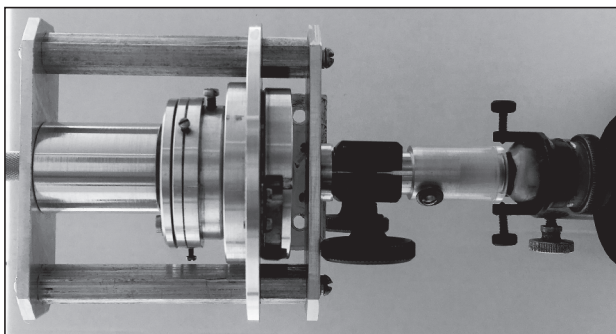


Figure 5. Ring converter of the laser beam intensity distribution.

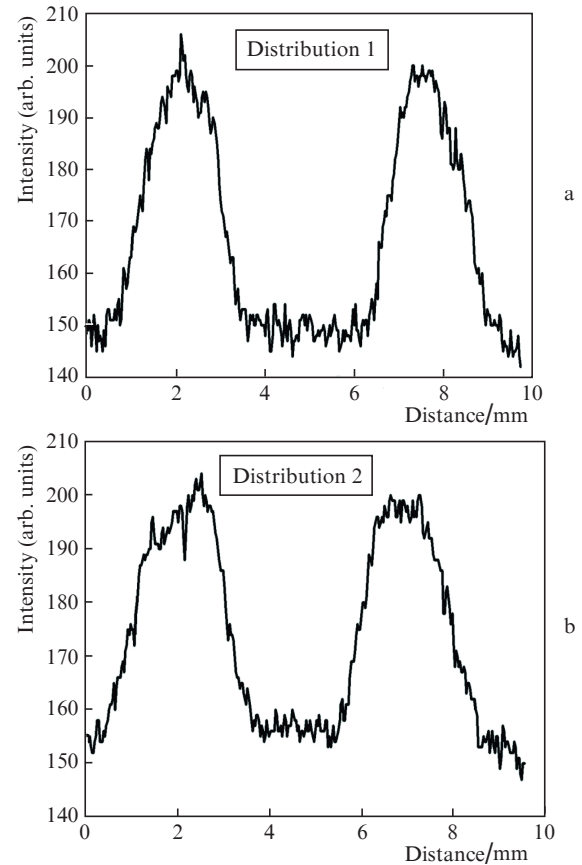


Figure 6. Cross sections of laser beam intensity distributions in the form of rings (a) 8.1 and (b) 8.5 mm in diameter, obtained with a fluorescent converter FID-AS-22.

and cw laser with output powers of 7.4 and 7.0 W respectively; the values of the integral radiation power in the ring at the converter output were, respectively, 1.3 and 1.2 W. The nonuniformity of the azimuthal intensity distribution did not exceed 5%, and the output power instability in the ring was 2.5% of the laser output power.

4. Experimental study of temperature fields on homogeneous objects

The radiation after the converter had an annular intensity distribution; the thickness and diameter of the ring could be controlled. We found and rigidly fixed two converter positions, which provided rings of two different diameters and thicknesses (see Fig. 6), with preservation of the same level of average intensity throughout the ring.

The irradiation of a spherical hydrogel phantom with a curvature radius corresponding to the curvature of human eye cornea external surface in the central optical region by an annular laser beam directed normally to the surface at the upper point of the sphere (Fig. 7) led to inhomogeneous but axisymmetric heating of the surface. The irradiation was performed in the repetitively pulsed regime: five 500-ms irradiation pulses separated by 300-ms intervals. An annular thermal field with a maximum temperature differing by 8°C from the ambient temperature was formed on the gel surface by the end of irradiation. The thermal field was symmetric relative to the center and had a dip of 5°C at the center. Since infrared imaging was performed at an

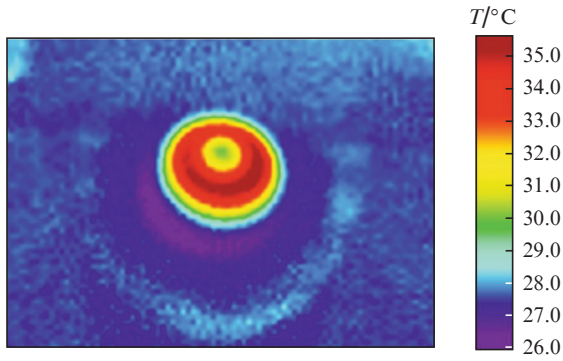


Figure 7. (Colour online) Temperature distribution on the surface of a gel phantom after its exposure to a laser beam with an annular intensity distribution (a ring 8.5 mm in diameter) at an average power of 7.4 W in the repetitively pulsed regime (5 pulses, pulse duration 500 ms, interval between pulses 300 ms).

angle of 60°, the temperature distribution in Fig. 7 is asymmetric relative to the irradiation axis.

Note that, to implement symmetric uniform heating of spherical samples, which is necessary for changing symmetrically the eye refraction, the laser beam was directed along the sphere axis, and the temperature was measured (using an infrared imager) at some angle to this axis. As a result, the recorded radial temperature distribution in the irradiated spot on the sphere surface was asymmetric because of the misalignment of the detection and beam axes (Fig. 8).

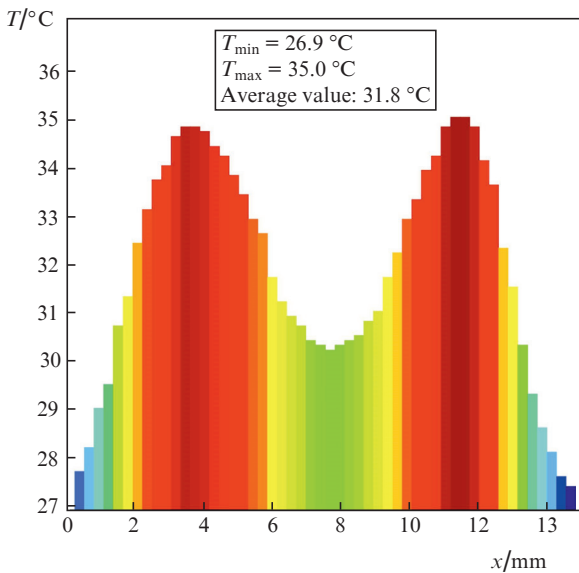


Figure 8. (Colour online) Radial temperature distribution over the laser irradiation spot on the surface of a gel sphere.

The thermal-field patterns on the surface of isolated rabbit eye under 5-s irradiation by annular laser beams with wide and narrow intensity distributions in the cw mode are presented in Fig. 9a; the corresponding temperature distributions are shown in Fig. 10.

It can be seen that, in the case of the wider ring, the temperature dip at the centre is larger and its maximum is

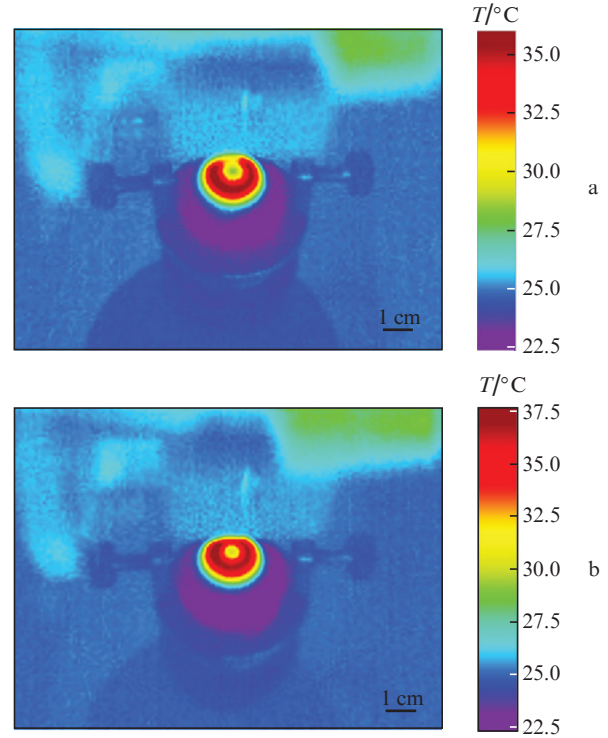


Figure 9. (Colour online) Thermal field patterns on the surface of isolated rabbit eye irradiated for 5 s by annular cw laser beams with (a) wide (ring 8.5 mm in diameter) and (b) narrow (8.1 mm) intensity distributions.

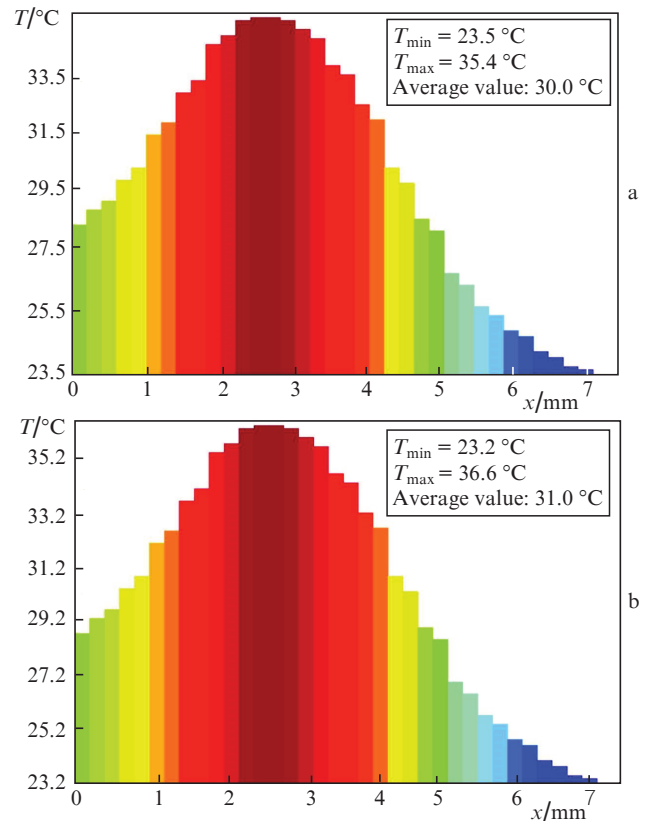


Figure 10. (Colour online) Radial temperature distributions over the surface of isolated rabbit eye in the laser beam spot: 5-s irradiation in the cw regime by an annular beam with an intensity distribution in a ring (a) 8.5 and (b) 8.1 mm in diameter.

shifted by a larger distance from the laser beam axis. It follows from the thermal patterns that the temperature distribution retains the form of a ring with a dip by 5–7°C at the centre during five pulses; upon cooling, the tendency of heat propagation with dip preserved at the centre is also retained (Fig. 11).

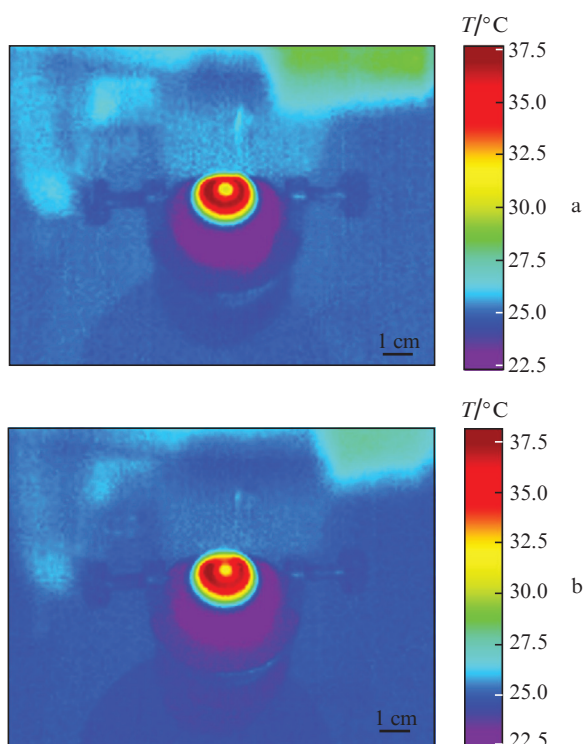


Figure 11. (Colour online) Thermal field patterns on the surface of isolated rabbit eye (a) at the end of irradiation by a laser beam with an annular intensity distribution 8.5 mm in diameter and (b) 2 s after switching off the laser.

The thermal field distribution formed on a spherical sample surface as a result of laser beam absorption (Fig. 10) is a true temperature distribution only in the vicinity of a surface element oriented normally to the infrared imager detector. In view of the sample surface curvature, this field is perceived by the infrared imager as distorted. On the one hand, an image becomes distorted under wide-aperture conditions. On the other hand, one can observe attenuation of the IR signal emitted by the surface elements making large angles with the detection direction. The consideration of the tilt angle of the surface to the optical system axis made it possible to measure the radial temperature distribution from the ring centre for a line on the surface lying in the observation plane. The distributions of the measured and calculated true heating temperatures of experimental samples for both irradiation intensity distributions are shown in Fig. 12.

To confirm the fact of symmetrical heating of spherical surfaces, we performed measurements in the multiangle view regime using a rotating camera. As a result, the thermal field in a spherical sample irradiated by an annular beam was verified to be symmetric relative to the beam axis.

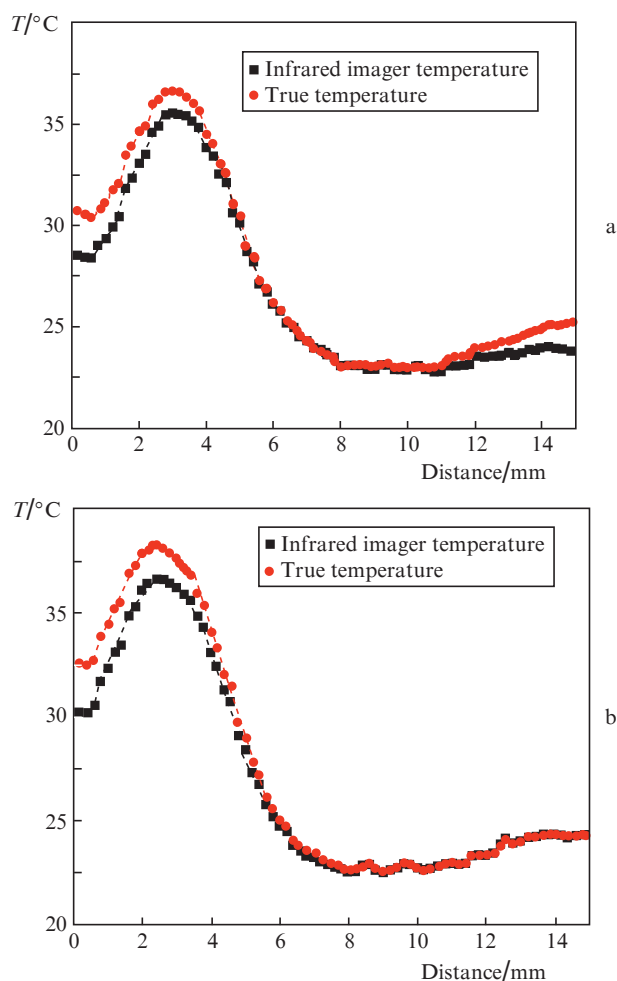


Figure 12. (Colour online) Radial distributions of measured (black curve) and calculated true (red curve) temperatures on the surface of isolated rabbit eye in the irradiation spot of a laser beam with an annular intensity distributions: rings (a) 8.5 and (b) 8.1 mm in diameter.

5. Conclusions

An algorithm was presented and the corresponding calculation was carried out in order to develop a laser emitter with an annular intensity distribution and homogenised spatial modes. The radiation intensity distributions and thermal fields on the eye surface in *ex vivo* experiments on non-ablative laser correction of the eye cornea profile were investigated for a device based on this algorithm. It is shown that this device can be used to implement a laser impact aimed at changing symmetrically the refraction of eye relative to its optical axis.

Acknowledgements. This study was supported by the Ministry of Science and Higher Education of the Russian Federation within the State Assignment for the Federal Scientific Research Centre ‘Crystallography and Photonics’ of the Russian Academy of Sciences.

References

1. Morozov V.I., Yakovlev A.A. *Farmakoterapiya glaznykh boleznei* (Pharmacotherapy of Eye Diseases) (Moscow: Meditsina, 2001).

2. Egorova T.S., Rozenblyum Yu.Z. *Refraktsionnaya Khir. Oftal'mologiya*, **2** (3), 12 (2002).
3. Kurenkov V.V. *Rukovodstvo po eksimerlazernoi khirurgii rogovitsy* (Guidance on Excimer Laser Surgery of Cornea) (Moscow: Izd-vo RAMN, 2002).
4. Bolshunov A.V., Gamidov A.A. *Lazernaya mikrokhirurgiya zrachkovykh membran* (Laser Microsurgery of Pupillary Membranes) (Moscow: Pamyatniki istoricheskoi mysli, 2008).
5. Sobol' E.N., Bolshunov A.V., Baum O.I., Zakharkina O.L., Omel'chenko A.I., Sipliviy V.I., Fedorov A.A. *Lazernye tekhnologii v oftal'mologii* (Laser Technologies in Ophthalmology). Ed. by S.E. Avetisov (Moscow: Aprel', 2013) Ch. 7.
6. Baum O.I., Bol'shunov A.V., Sipliviy V.I., Ignat'eva N.Y., Zakharkina O.L., Lunin V.V., Myakov A.V. *Laser Phys.*, **16**, 5 (2006).
7. Bolshunov A., Sobol E., Avetisov S., Baum O., Siplivy V., Omelchenko A., Fedorov A. <https://doi.org/10.1111/j.1755-3768.2011.2172.x>.
8. Baum O.I., Yuzhakov A.V., Bolshunov A.V., Sipliviy V.I., Khomchik O.V., Zheltov G.I., Sobol' E.N. *Quantum Electron.*, **47** (9), 860 (2017) [*Kvantovaya Elektron.*, **47** (9), 860 (2017)].
9. Zaitsev V.Y., Matveyev A.L., Matveev L.A., Gelikonov G.V., Omelchenko A.I., Baum O.I., Sobol E.N. *J. Biophotonics*, **10** (11), 1450 (2017); doi:10.1002/jbio.201600291.
10. Zaitsev V.Y., Matveyev A.L., Matveev L.A., et al. <https://doi.org/10.1002/jbio.201800250>.
11. Zaitsev V.Y., Matveev L.A., Matveyev A.L., Sovetsky A.A., Shabanov D.V., Ksenofontov S.Y., Sobol E.N. *Laser Phys. Lett.*, **16** (6), 065601 (2019).
12. Baum O.I., Bolshunov A.V., Omel'chenko A.I., Poleva R.P., Sipliviy V.I., Sobol' E.N. *Al'manakh klinicheskoi meditsiny* (Anthology of Clinical Medicine) (Moscow, 2008) Vol. XVII, Part 1, pp 32–34.
13. Klopfer M., Block M.K., Deffenbaugh J., et al. *Proc. SPIE*, **10090**, 100901N (2017).
14. Nemeč M., Indra L., Šulc J., Jelínková H. *Proc. SPIE*, **9726**, 97261B (2016).
15. Golub M.A., Kazanskii N.L., Sisakyan I.N., Soifer V.A., Kharitonov S.I. *Optoelectronics, Instrumentation and Data Processing*, **6**, 7 (1987).
16. Doskolovich L.L., Kazansky N.L., Kharitonov S.I., Soifer V.A. *J. Mod. Opt.*, **43** (7), 1423 (1996).
17. Doskolovich L.L., Kazanskij N.L., Pavel'ev V.S., Sojfer V.A. *Avtometriya*, **1**, 114 (1995).
18. Kang G.-G., Xie J.-H., Mo X.-L., Wang D.-F., Zhang H., Guangzi Xuebao. *Acta Photonica Sinica*, **37** (7), 1416 (2008).
19. Bykov D.A., Doskolovich L.L., Mingazov A.A., Bezus E.A., Kazanskiy N.L. *Opt. Express*, **26**, 27812 (2018).
20. Gerchberg R.W., Saxton W.O. *Optik*, **35** (2), 237 (1972).
21. Fienup J.R. *Appl. Opt.*, **21** (15), 2758 (1982).
22. Kazanskiy N.L., Kotlyar V.V., Soifer V.A. *Opt. Eng.*, **33** (10), 3156 (1994).
23. Kharitonov S.I., Doskolovich L.L., Kazanskiy N.L. *Computer Opt.*, **40** (4), 439 (2016).
24. Kazanskiy N.L., Kharitonov S.I., Kozlova I.N., Moiseev M.A. *Computer Opt.*, **42** (4), 574 (2018).